Citation: Journal of the Optical Society of America A Vol. 24, Issue 12, pp. 3691-3699 (2007)
https://doi.org/10.1364/JOSAA.24.003691

The optical constants of Yb films in the 23-1,700 eV range

Mónica Fernández-Perea[1], Juan I. Larruquert[1,*], José A. Aznárez[1], José A. Méndez[1]

Luca Poletto[2], Denis Garoli[2]

A. Marco Malvezzi[3]

Angelo Giglia[4], Stefano Nannarone[4]

[1]GOLD: Grupo de Optica de Láminas Delgadas, Instituto de Física Aplicada-Consejo Superior de Investigaciones Científicas

Serrano 144, 28006 Madrid, Spain

[2]Istituto Nazionale per la Fisica della Materia-CNR & Dep. of Information Engineering, Padua, Italy

[3]Dipartimento di Elettronica, Università di Pavia and INFM, Via Ferrata, 1, I27100 Pavia, Italy

[4]Laboratorio TASC-INFM-CNR, S.S. 14, km 163.5 in Area Science Park, I-34012 Trieste, Italy

[*]Corresponding author: larruquert@ifa.cetef.csic.es

The optical constants of Yb films have been determined in the 23-1,700 eV spectral range from transmittance measurements performed in situ on Yb films deposited by evaporation in ultra high vacuum (UHV) conditions. Yb films were deposited over grids coated with a thin carbon film. Transmittance measurements were used to obtain the extinction coefficient of Yb films at each individual photon energy investigated. The energy range investigated encompasses Yb edges from $M_{4,5}$ to $O_{2,3}$. The current results, along with data in the literature, show that Yb has an interesting low-absorption band in the ~12-24 eV range which may be useful for the development of transmittance filters and multilayer coatings. The current data along with literature data and extrapolations were used

to obtain *n*, the real part of the complex refractive index, using a Kramers-Krönig analysis. The application of the sum-rules showed a good consistency of the results.

OCIS Codes: 260.7200 Ultraviolet, extreme; 120.4530 Optical constants; 350.2450 Filters, absorption; 230.4170 Multilayers; 310.6860 Thin films: optical properties

1. Introduction

The optical constants of many materials, such as most lanthanides, have not yet been measured in parts of the extreme ultraviolet (EUV, ~10-1,000 eV) and x-rays. In addition to the intrinsic difficulty of optical characterization of materials in the EUV, the lanthanides are very reactive under normal atmosphere. Ultra high vacuum (UHV) conditions are therefore required for a meaningful characterization. This paper addresses the optical properties of Yb in the EUV, and it aims at filling the lack of data in important parts of the EUV. The following literature is available on the optical properties of Yb in the EUV. Endriz and Spicer[1] measured the reflectance of Yb and other materials in the 1-11.5 eV range, and they deduced the dielectric constant and other functions; their research was performed in situ in UHV conditions, with extreme care in the sample handling. Larruquert et al.[2] measured the reflectance as a function of the angle of incidence and the transmittance of Yb films deposited in situ in UHV conditions; they obtained the optical constants of Yb in the range 7.1-23.1 eV, which matched acceptably well those of Endriz and Spicer in the region of coincidence. Even though the available measurements do not cover the full range of interest, Yb films have been shown to have promising filtering properties in the EUV[2]. This makes Yb a candidate material for filters and multilayers in the ~12-24-eV spectral range, where few materials with a relatively low absorption, such as In and Sn, are available. At larger energies, Gribovskii and Zimkina[3] measured the absorption coefficient of Yb and other lanthanides in the 70-500 eV range; Yb films were protected

with an Al film, and, apparently, the authors measured the sample transmittance in situ. In our literature search, no measurements of the extinction coefficient of Yb were found in the regions 23.1-70 and above 500 eV, and no data on the refractive index above 23.1 eV was found.

This paper reports on the characterization of Yb films in the spectral range from 23 to 1,700 eV and on the determination of Yb optical constants in the above range. A similar research has been recently performed on Sc films with the same methodology and experimental techniques[4]. The extinction coefficient (k) of Yb films was obtained from transmittance measurements and the refractive index (n) was calculated with the Kramers-Krönig analysis using the current data along with those in the whole spectrum derived from the literature and from extrapolations. An advantage of this method is that there is no dependence on radiation polarization because of measurements are performed at normal incidence. Furthermore, the dependence on surface scattering is considerably smaller than with other techniques such as reflectance measurements, because only transmittance versus thickness is handled, and roughness terms common to films with different thicknesses can be cancelled out; roughness dependence is also minimized at large energies because roughness-induced transmittance reduction is governed by n-1 (refractive index difference between the film and the incidence medium), which approaches zero with increasing photon energy. The present technique is also simple compared to ellipsometry, which has not fully developed in the EUV due to the difficulty in making efficient polarizers. The experimental techniques used are described in Section 2. Section 3 reports experimental data, KK analysis, evaluation of the consistency of the data, and surface analysis to evaluate the contamination of the samples.

2. Experimental techniques

2.1 SAMPLE PREPARATION

Yb films were deposited over substrates that consisted of a thin carbon film that was supported on a microgrid. We used electroformed hexagonal nickel grids of 750 mesh (hole: 25 μm; bar: 8 μm, thickness: ~8 μm) with a transmittance of about 50%. C films of ~10-nm thickness were deposited by evaporation with an electron gun. The C film was deposited on a microgrid coated with a collodion film; the latter was later dissolved in amyl acetate.

A total number of five Yb layers were deposited. Two substrates received two Yb layer depositions, and the transmittance was measured both for the plain substrate and after each deposition. A third substrate received one single layer of Yb. The samples were transferred back and forth between the deposition chamber and the measurement chamber, always under UHV, for the deposition of the first or second Yb layer and for its characterization. We used a TriCon evaporation source[5], in which Yb lumps of 99.9% purity from Sigma-Aldrich were placed in a Ta crucible that was heated by the electrons coming from a surrounding filament. The substrates were placed at room temperature for Yb deposition. The distance from the source to the substrate was 10 cm. Deposition rate was maintained at ~0.1 nm/s for all the evaporations. Film thickness was monitored with a quartz crystal monitor during deposition. The real thickness of each layer was obtained by fitting the transmittance versus photon energy with Henke data[6] in a selected energy range. The latter were downloaded from the website of the Center for X-Ray Optics (CXRO) at Lawrence Berkeley National Laboratory[7].

2.2 EXPERIMENTAL SETUP FOR TRANSMITTANCE AND PHOTOEMISSION MEASUREMENTS

The transmittance measurements were performed at the BEAR beamline at Elettra Synchrotron (Trieste, Italy), which operates in the energy range from 3 to 1,700 eV, and consists of a monochromator and two experimental stations, one for the preparation of the samples and one for the measurements. The monochromator has three different channels with gratings that are illuminated in parallel light, two of them with optics at grazing incidence and one at normal incidence.

The spectral range was covered with two channels: the NIM (Normal-Incidence Monochromator) channel, working at fixed deviation angle to cover the 20-50 eV energy range, and the G1200 channel, working at grazing incidence and at selectable deviation angle to cover the 40-1,700 eV range[8]. Taking into account that transmittance measurements at normal incidence are independent of the degree of polarization of light for isotropic materials, we measured with full beam, which results in a degree of linear polarization of about 0.5[9]. With the used slit configuration, the monochromator spectral broadening was ~0.1 eV in the range 20-200 eV and ~0.5 eV in the range 200-1,700 eV. The suppression of higher orders was achieved by using Al and Si filters below 100 eV, and by selecting the optimum deviation angle at higher energies. The spot size on the sample was 0.4x0.2 mm^2, as given by the used exit slits aperture. With this slit configuration, the monochromator spectral broadening is ~0.01 eV in the range 20-50 eV, ~0.1 eV in the range 50-300 eV, ~1 eV in the range 300-1,700 eV. The uncertainty in the photon energy calibration was below 0.5 eV.

The measurements were performed at the BEAR spectroscopy chamber[10] ($P=8x10^{-8}$ Pa), connected in vacuum to the preparation chamber ($P=2x10^{-8}$ Pa), where in-situ samples were prepared. The direct I_D and transmitted I_T signals were measured using an IRD SXUV-100 silicon photodiode detector. The

correction of the background signal was done by measuring the dark signal I_B of the photodiode, and possible fluctuations of the photon beam during measurements were recorded using the current R generated by a 100-V biased W-mesh on the input beam. The normalization of the measurements was then performed through:

$$T = \frac{(I_T - I_B)/(R_T - R_B)}{(I_D - I_B)/(R_D - R_B)} \quad (1)$$

where R_T and R_D and R_B represent the mesh currents measured during transmittance, direct beam and dark measurements, respectively.

Photoemission measurements were performed in the BEAR spectroscopy chamber in order to characterize the surface of three Yb films. The electron analyzer was a Spherical Deflector Analyser (SDA) with an input system based on three lenses and working in a kinetic energy range of 1-1,000 eV. The maximum accepted solid angle was 4×10^{-4} sr, corresponding to a cone aperture semiangle of 2º, and the field of view was 0.2×2 mm^2 (spectral × spatial).

In order to characterize the chemical state of the surface of the 2nd, 3rd, 4th Yb films, photoemission measurements were performed in the measurement chamber just after transmittance with an electron analyzer whose specifications are given in Ref. [10].

3. Results and discussion

3.1 TRANSMITTANCE AND EXTINCTION COEFFICIENT OF Yb

Prior to transmittance measurements, the uniformity of the substrate was verified inside the central region of the sample (4×4 mm^2). For each film we verified the uniformity at the photon energy of 200 eV; the variation of transmittance signal was less than 2%. The sample was positioned for all the

measurements in the same position within an uncertainty of 0.5 mm. We can estimate that the overall uncertainty in the transmittance measurements was of the order of 2%.

The transmittance of five Yb films was measured. Preliminary thickness measurements of the films were performed in real time with a quartz crystal monitor. Since in situ facilities for thickness measurement or film protection were not available, witness substrate for thickness determination were not mounted. Instead, final thickness values were obtained by fitting the current transmittance with Henke data between the $N_{4,5}$ and the $M_{4,5}$ edges. Before the fittings to Henke data, the density of Yb films was measured. To do this we deposited a 160-nm thick Yb film onto an Al foil in a high vacuum evaporator at GOLD, in which we reproduced the geometry and the deposition rate of the depositions at the beamline. We weighed the Al foil both before and after Yb deposition using scales with a precision of ±0.01 mg. The thickness of the Yb film was measured by Tolansky interferometry on a witness sample. We measured the surface area of the deposit with an optical comparator. We obtained an Yb density of 6.81±0.17 g/cm^3. This value may be compared with 6.903 and 6.966 g/cm^3 for bulk α and β crystalline Yb, respectively. The density of the film is slightly smaller than that of bulk Yb, although the density of bulk Yb is contained within the uncertainty interval.

The Yb layer thicknesses so obtained were 32, 47, 51, 85, and 114 nm. The transmittance of the samples normalized to that the uncoated substrate is plotted in Fig. 1. The normalized transmittance of two of these films is extended in Fig. 2 to smaller photon energies using data measured in Ref. [2] for films of close thickness. A low-absorption band is observed in the 12-24 eV range. The gaps between plots can be explained by the slight thickness differences. Yb transmittance in the EUV makes this material a promising candidate as a filter with a high transmittance region in the ~12-24 eV. However, Yb was shown to have strong ageing effects[2]; the transmittance of Yb films was seen to decay even under UHV, and the decay did not slow down completely after 5 days of storage

in a desiccator. The transmittance decay was attributed to a combination of hydridation and oxidation. The shape of the aged sample transmittance was similar to that of fresh Yb, which suggests that an unprotected Yb filter would maintain the relative transmittance efficiency for the different energies roughly constant over time. Protective layers need to be developed in order to prevent Yb from reacting with normal atmosphere or with the residual gases of a vacuum chamber or of a terrestrial orbit for in-space astronomy. Yb high reactivity leaves open the key problem to find a protective material for Yb with adequate transmittance. Another interesting application of Yb may be as a material for reflective multilayers within Yb low-absorption band, as long as a stable outermost coating with adequate optical constants is available.

We now obtain the extinction coefficient *k* of Yb from the transmittance measurements. Transmittance is related to *k* through:

$$\frac{T_{fs}}{T_s} \approx \exp\left(-\frac{4\pi k x}{\lambda}\right) \tag{2}$$

where T_s and T_{fs} represent the transmittance of the uncoated substrate and of the substrate coated with an Yb film, respectively. λ is the radiation wavelength in vacuum. *x* stands for the Yb film thickness. Eq. (2) neglects the reflectance of the layer at both interfaces. The largest normal incidence reflectance of the Yb films has been estimated to be lower than ~2% for energies between 23 and 60 eV, and lower than ~0.1% above 60 eV. Neglecting reflectance in the calculation of the extinction coefficient from transmittance measurements adds then a negligible error.

k at each energy was calculated by fitting the slope of the logarithm of transmittance versus thickness using Eq. (2). Examples of transmittance measurements for 5 different photon energies are given in Fig. 3. Almost the whole set of Yb transmittance was used to calculate *k*. Only the

measurements between 23 and 40 eV performed over the two thickest samples were discarded since the transmitted signal was low and hence the contribution of second order was not negligible.

Fig. 4 represents the extinction coefficient versus the photon energy obtained for Yb. The data of Gribovskii et al.[3] and Henke et al.[6] are also displayed for comparison purposes. Gribovskii data match well the current data. The main difference arises in that Gribovskii data have a small peak centered at 180 ± 5 eV, which is not seen in the current data. This difference can be explained[11] by a hypothetical higher degree of oxidation of Gribovskii samples, which were deposited in poorer vacuum conditions (~10^{-3} Pa during film growth). Henke data presented in this paper were calculated with the density measured in the present investigation.

The covered spectral range spans from $M_{4,5}$ to $O_{2,3}$ edges of Yb. Fits were obtained for sub-ranges limited by Yb edges. Henke et al.[6] referred to the work of Biggs and Lighthill[12], where fits between edges were performed with four-order polynomial of the inverse of energy. We provide in Table 1 fits for the sub-ranges between edges $M_{4,5}$ and N_4 and between N_4 and $O_{2,3}$. An energy term with a positive power had to be included in the 48-190 eV to better fit the large energy limit. The empty boxes mean that such a term was not used in the fitting. $M_{4,5}$ edge and the broad $O_{2,3}$ edge is clearly visible in Fig. 4.

Fig. 5 represents the current *k* data around and below $O_{2,3}$ edge, along with the data of Refs. 1 and 2. The connection between the two sets of measurements is excellent. A low absorption band in the ~12-24 eV can be observed, with lowest absorption at 21.2 eV. The data in Ref. [2] did not plot the whole low-absorption band, which is completed with current data. At present only filters of In and Sn are available with low-absorption bands at ranges close to that of Yb. In and Sn main transmittance regions are ~11.8-16.5 eV nm and ~15.5-24.8 eV, respectively. Hence, the main transmittance region of Yb

roughly combines the transmittance regions of In and Sn, but, as reported in Ref. [2], Yb has a lower rejection below ~12.4 eV.

Fig. 6 highlights *k* data around $M_{4,5}$ edge along with Henke data[6]. The two sets of data are considerably different, but it is well known that the semi-empirical data of Henke et al. are not accurate at the absorption edges. M_4 and M_5 edges cannot be observed separately in the figure.

3.2 REFRACTIVE INDEX CALCULATION WITH THE DISPERSION RELATIONS

The dispersion of Yb was calculated using the KK dispersion relations:

$$n(E) - 1 = \frac{2}{\pi} P \int_0^{\infty} \frac{E' k(E')}{E'^2 - E^2} dE' \qquad (3)$$

where *P* stands for the Cauchy principal part. The application of Eq. (3) to calculate *n* requires the availability of *k* data over the whole spectrum. Since the determination of *k* on a specific sample in the whole spectrum is not possible, KK analysis requires gathering data coming from different sources, different sample preparation, etc., which results in inaccuracies when calculating *n* with Eq. (3).

The most reliable data that are available for Yb encompass the current data, along with the in situ data of Endriz and Spicer[1] and Larruquert et al.[2], which have been referred to above; they result in a total range of 0.3-1,700 eV in which *k* was measured in situ. Regarding other small photon energy data, Idczak and Żukowska[13] measured reflectance in the 0.05-6.2 eV range apparently ex situ, and they calculated the optical constants of Yb using the KK dispersion relations. Müller[14] measured reflectance of Yb films in the 0.3-5 eV range through sapphire windows on which an Yb film had been evaporated. Pétrakian[15] measured the reflectance and transmittance of Yb films in which it is not clear whether the samples were or were not exposed to atmosphere before optical measurements; from them, the conductivity was calculated. Chander and Kumar[16] measured the optical density of Yb

films protected with a thin film of LiF in the 0.83-10.3 eV; they observed the influence of the Yb film thickness on the position of the optical density peaks. Endriz and Spicer[1] compared their reflectance to the work of Müller, and the latter was considerably lower; however, since Müller's reflectance was apparently measured on the sapphire-Yb interface, Müller's data cannot be compared directly with Endriz's data. The reflectance data of Idczak and Zukowska are even considerably lower than those of Müller. Furthermore, the extinction coefficient provided by Idczak and Zukowska was a factor of ~0.7 times that of Endriz and Spicer in the coincidence region. Since possible oxidation or other reactions of Yb are expected to result in reflectance decay when reflectance is not small and the work of Endriz and Spicer was performed in situ under optimum vacuum conditions, the latter work looks more reliable. The work of Pétrakian does not provide *k*. We also calculated the conductivity using the data of Endriz and Spicer and compared them to Pétrakian's and Müller's data, and again the match was not good. Due to all the above, the work of Müller, Pétrakian, and Idczak and Zukowska were discarded in the construction of a full set of *k* data. Consequently, the data of Larruquert et al. were used from 23 down to 8.3 eV, below which the data of Endriz and Spicer were used down to 0.3 eV, and an extrapolation with a free electron model was performed down to 0 eV.

Between 1,700 and $3x10^4$ eV we used Henke data from CXRO's web[7], which provides *k* data encompassing Yb $L_{1,2,3}$ edges. For even larger energies, the calculations of Chantler et al.[17] were used up to $4.3x10^5$ eV, which provides *k* data encompassing Yb K edge. The extrapolation to infinity was performed by keeping constant the slope of the log-log plot of $k(E)$ in the Chantler data [17]. The extrapolation curve depended on energy as $E^{-3.47}$. Fig. 7 displays the *k* data of Yb that were gathered for the KK analysis.

Figs. 8 to 10 display $\delta=1-n$ calculated with Eq. (3) using data plotted in Fig. 7. Fig. 8 shows some difference with Henke data below ~200 eV. In Fig. 9 we can see a good coincidence of δ between

the current calculation and the data of Larruquert et al.[2] except for the smallest energy value of Ref. [2]. The coincidence is less good with Endriz data, except for the latter's largest energies, even though at 8.3 eV and below the data of Ref. [1] were used in the KK analysis. At $M_{4,5}$ edge, Fig. 10 shows a large difference between the current data and those of Henke, and again, the difference is explained through the lower accuracy of Henke model at the absorption edges. Fits of δ for the sub-ranges between edges $M_{4,5}$ and N_4 and between N_4 and $O_{2,3}$ are also displayed in Table 1.

The *f*-sum rule test provides a valuable guidance to evaluate the accuracy of the *k* data; it relates the number density of electrons to the dissipative or imaginary part *k(E)* of the refractive index[18]. This sum-rule can be written as:

$$\int_0^\infty E\,k(E)\,dE = \frac{\pi N_{el} e^2 h^2}{4\varepsilon_0 m} \tag{4}$$

where N_{el} is the electron density, *e* is the electron charge, ε_0 is the permittivity of vacuum, *m* is the electron mass, and *h* is Planck's constant. It is useful to define the effective number of electrons contributing to the optical properties up to a given energy as:

$$n_{eff}(E) = \frac{4\varepsilon_0 m}{\pi N_{at} e^2 h^2}\int_0^E E'\,k(E')\,dE' \tag{5}$$

where N_{at} is the atom density. In the limit of high energy n_{eff} must converge to the number of electrons of an Yb atom. The international system of units is used here, whereas CGS was used in Ref. [18], which explains the differences in Eqs. (4) and (5) with those of Ref. [18].

For Yb, the high-energy limit of the effective number of electrons must reach *Z*=70. When the relativistic correction on the scattering factors is taken into account, the high-energy limit of Eq. (5) is

slightly modified. Henke et al.[6] fitted relativistic correction data of Kissel and Pratt[19] with the following function:

$$Z^* = Z - \left(Z/82.5\right)^{2.37} \tag{6}$$

where Z^* is the modified atomic number to be used in *f*-sum rule instead of *Z*. This correction for Yb results in Z*=69.32.

A high-energy limit of 70.27 was obtained for n_{eff} by integration of the *k* data displayed in Fig. 7. This value is only 1.4% larger than the above Z^* value. This small deviation on the *f*-sum rule test, which is smaller than the expected experimental uncertainty of the extinction coefficient of Yb, shows a good consistency of *k* data.

A useful test to evaluate the accuracy of the KK analysis is obtained with the inertial sum-rule:

$$\int_0^\infty \left[n(E) - 1\right] dE = 0 \tag{7}$$

which expresses that the average of the refractive index throughout the spectrum is unity. In practice it must be defined some way of evaluating whether the calculated integral of Eq. (7) is or is not close enough to zero. Shiles et al.[18] proposed the following evaluation parameter:

$$\zeta = \frac{\int_0^\infty \left[n(E) - 1\right] dE}{\int_0^\infty \left|n(E) - 1\right| dE} \tag{8}$$

Shiles et al.[18] used the above parameter in the analysis of Al and obtained ζ=-0.002. They mentioned some other work on Al in which ζ takes a value as high as 0.17, which demonstrates a large inconsistency of the analysis. They suggested that a good value of ζ should stand within

±0.005. The sum-rule test in the present case resulted in ζ=-0.0027, which is well within the top value proposed by Shiles et al.

3.3 SURFACE ANALYSIS

Photoemission measurements have been performed in order to analyze the degree of contamination of the surface of three of the Yb films deposited on C substrates. Fig. 11 shows three different spectra, performed at the fixed photon energy of 650 eV, and with pass energy of 50 eV corresponding to analyzer resolution of 0.5 eV. Inspection of Fig. 11 shows the core level peaks of O K at ~110 eV, Yb N_3 at ~305 eV and Yb N_{45} at ~455 eV. Moreover, the Auger peaks of O KLL at ~510 eV and the Yb $N_{45}N_{67}N_{67}$ at ~170 eV are also present. Hence, these photoemission spectra show the presence of oxygen on the film surface. Instead, there is no significant evidence of carbon contamination. The thickness of ytterbium oxide on the surface was calculated by comparing the O K and Yb N_{45} photoemission peak areas, following the model described in Ref. [20]. The peak area was calculated after Shirley background subtraction[21]. In the calculation we assumed that the sample was a homogeneous Yb_2O_3 film of *d* thickness over an Yb substrate. For Yb we assumed the measured density, while for the oxide we used the bulk density of 9.2 g/cm^3. Moreover, we took into account the cross section of the two core levels σ_{OK} and σ_{YbN}, the electron mean free path Λ and the transmission of the electron analyzer at two relative kinetic energies T_{YbN} and T_{OK}[8]. At the end, the thickness of oxide is given by

$$d = \frac{\left(\frac{R_{YbN} A_{Yb} T_{YbN} \Lambda_{YbN}}{\sigma_{YbN}}\right)}{\left(\frac{\sigma_{OK} R_{YbN} T_{OK} \Lambda_{OK}}{\sigma_{YbN} A_{Yb}}\right) + \left(\frac{R_{YbN} \Lambda_{YbN}}{A_{Yb}}\right)} \qquad (10)$$

where R is the ratio between the O K and Yb N core line areas, c_O (c_{Yb}) is the atomic fraction of oxygen (ytterbium) in the Yb_2O_3 molecule and A_O (A_{Yb}) stands for the atomic weights of oxygen (ytterbium). The calculated thickness of the oxide is between 0.3 and 0.4 nm for the three samples: the degree of contamination due to the exposure to the residual atmosphere is then of the order of ~1 oxygen layer. This thickness can be considered negligible for the transmission measurements through some tens of nanometers of metallic ytterbium. Furthermore, the photoemission measurements were performed at the end of the transmittance measurements, so that the latter were performed most probably with a smaller amount of oxide than the above.

A more accurate investigation of the valence band states has been performed. Fig. 12 represents the outermost levels of the Yb samples, obtained at the photon energy of 150 eV and with an analyzer resolution of 0.1 eV. The two main peaks at binding energies of about 1.5 and 3 eV can be ascribed respectively to the final state multiplets N_7 and N_6 of the clean Yb[11]. On the other hand, the two shoulders located 0.5 eV towards higher energies with respect to the just mentioned Yb peaks are surface emissions[22]. The inspection of the figure reveals moreover two little broadened peaks at about 8-9 and 12-13 eV that can be ascribed to final state multiplets relative to oxidized Yb (in particular the peak at 8.5 eV refers to O L emission of Yb_2O_3). A qualitative inspection of the valence band, compared with the spectra of the clean metal or after 100 Langmuirs of O2 exposure (1 Langmuir=1.33×10^{-4} Pa×s), shown in Ref. [11], confirms that the samples are only slightly contaminated by residual gas. The photoemission spectra of the three samples and then also the chemical states are similar; only the second evaporation on the second sample shows a slightly higher degree of contamination.

CONCLUSIONS

The transmittance of thin films of Yb deposited by evaporation has been measured in situ in the 23-1,700 eV photon energy range in UHV conditions. The transmittance measurements have been used to calculate the extinction coefficient of pure Yb in the same spectral range. Yb has a low-absorption band in the 12-24 eV range peaked at 21.2 eV, which makes Yb a promising candidate for transmittance filters and reflective multilayers. The key problem of Yb passivation without destroying its EUV properties is still open.

The refractive index of Yb in the same energy range has been calculated through the KK dispersion analysis, using the current data along with the data available in the literature. All data used above 0.3 eV come from measurements performed in situ in UHV conditions, except above 1,700 eV, where the Henke semi-empirical approach was used.

The *f*-sum rule resulted in a value only 1.4% above the theoretical one, which shows a good consistency of the current *k* data along with the data in the literature that were gathered. The evaluation of the inertial sum-rule resulted in a good consistency of the KK dispersion analysis.

ACKNOWLEDGMENTS

We acknowledge support by the European Community - Research Infrastructure Action under the FP6 "Structuring the European Research Area" Programme (through the Integrated Infrastructure Initiative "Integrating Activity on Synchrotron and Free Electron Laser Science"). This work was also supported by the National Programme for Space Research, Subdirección General de Proyectos de Investigación, Ministerio de Ciencia y Tecnología, project numbers ESP2001-4517-PE, ESP2002-01391, ESP2005-

02650, and ESP2005-25299-E. A. M. M. acknowledges the partial support of the Fondo d'Ateneo per la Ricerca (FAR) of Università di Pavia. M. F. is thankful to Consejo Superior de Investigaciones Científicas (Spain) for funding under the Programa I3P (Ref. I3P-BPD2004), partially supported by the European Social Fund. The technical assistance of J. M. Sánchez-Orejuela is acknowledged.

REFERENCES

[1]. J. G. Endriz, W. E. Spicer, "Reflectance studies of Ba, Sr, Eu, and Yb", Phys. Rev. B **2**, 1466-1492 (1970).

[2]. J. I. Larruquert, J. A. Aznárez, J. A. Méndez, José Calvo-Angós, "Optical properties of Yb films in the far and the extreme ultraviolet", Appl. Opt. **42**, 4566-4572 (2003).

[3]. S. A. Gribovskii, T. M. Zimkina, "Absorption coefficients of rare-earth elements of the lanthanum group in the ultrasoft X-ray region", Opt. Spectrosc. **35**, 104-105 (1973).

[4]. M. Fernández-Perea, J. I. Larruquert, J. A. Aznárez, J. A. Méndez, L. Poletto, A. M. Malvezzi, A. Giglia, S. Nannarone, "Determination of optical constants of scandium films in the 20-1000 eV range", J. Opt. Soc. Am. A **23**, 2880-2887 (2006).

[5]. R. Verucchi, S. Nannarone, "Triode electron bombardment evaporation source for ultrahigh vacuum thin film deposition", Rev. Sci. Instrum. **71**, 3444-3450 (2000).

[6]. B.L. Henke, E.M. Gullikson, and J.C. Davis, "X-ray interactions: photoabsorption, scattering, transmission, and reflection at E=50-30000 eV, Z=1-92", Atomic Data and Nuclear Data Tables **54**, 181-342 (1993).

[7]. http://www-cxro.lbl.gov/optical_constants/

[8]. S. Nannarone, F. Borgatti, A. De Luisa, B. P. Doyle, G. C. Gazzadi, A. Giglia, P. Finetti, N. Mahne, L. Pasquali, M. Pedio, G. Selvaggi, G. Naletto, M. G. Pelizzo, G. Tondello, "The BEAR beamline at ELETTRA", T. Warwick, J. Arthur, H. A. Padmore, J. Stöhr, eds., *AIP Conference Proceedings **705***, 450-453 (2004).

[9]. M.-G. Pelizzo, F. Frassetto, P. Nicolosi, A. Giglia, N. Mahne, S. Nannarone, “Polarization and higher order content measurement of a soft-x-rays monochromatized beam with Mo/Si multi-layers”, *Applied Optics 45, 1985 (2006).*

[10]. L. Pasquali, A. De Luisa, S. Nannarone, “The UHV Experimental Chamber For Optical Measurements (Reflectivity and Absorption) and Angle Resolved Photoemission of the BEAR Beamline at ELETTRA”, T. Warwick, J. Arthur, H.A. Padmore, J. Stöhr, eds., *AIP Conference Proceedings **705***, 1142-1145 (2004).

[11]. L.I. Johansson, J.W. Allen, I. Lindau, M.H. Hecht, S.B.M. Hagstrom, “Photoemission from Yb: Valence-change-induced Fano resonances”, Phys. Rev. B **21**, 1408-1411 (1980).

[12]. F. Biggs and R. Lighthill, "Analytical Approximations for X-Ray Cross Sections", Part II, SC-RR-710507, Sandia Laboratories, Albuquerque, New Mexico, 1971, as cited by B. L. Henke, P. Lee, T. J. Tanaka, R. L. Shimabukuro, B. K. Fujikawa, Atomic Data and Nuclear Data Tables **27**, No. 1, 1-144 (1982).

[13]. E. Idczak, K. Żukowska, “Optical properties and microcharacteristics of thermally evaporated Ytterbium films”, Thin Solid Films **75**, 139-142 (1981).

[14]. W. E. Müller, “Optical properties of divalent rare-earthmetals and alkaline-earth metals”, Phys. Lett. **17**, 82-83 (1965).

[15]. J. P. Pétrakian, “Conductivité at transitions optiques dans des couches minces d’ytterbium”, Thin Solid Films **20**, 297-305 (1974).

[16]. R. Chander and R. Kumar, “Optical absorption in vacuum-evaporated ytterbium films”, Phys. Stat. Sol. (a) **20**, 739-744 (1973).

[17]. C. T. Chantler, K. Olsen, R. A. Dragoset, J. Chang, A. R. Kishore, S. A. Kotochigova, D. S. Zucker, “X-Ray Form Factor, Attenuation and Scattering Tables” (version 2.1), (2005). [Online] Available: http://physics.nist.gov/ffast [2006, May 29]. National Institute of Standards and

Technology, Gaithersburg, MD. Originally published as C. T. Chantler, J. Phys. Chem. Ref. Data **29**, 597-1048 (2000); and C. T. Chantler, J. Phys. Chem. Ref. Data **24**, 71-643 (1995).

[18]. E. Shiles, T. Sasaki, M. Inokuti, D. Y. Smith, "Self-consistency and sum-rule tests in the Kramers-Kronig analysis of optical data: applications to aluminium", Phys. Rev. B **22**, 1612-1628 (1980).

[19]. L. Kissel, R. H. Pratt, "Corrections to tabulated anomalous-scattering factors", Acta Cryst. **A46**, 170-175 (1990).

[20]. C. D. Wagner, W. M. Riggs, L. E. Davis, J. F. Moulder, G. E. Muilenberg, "Handbook of photoelectron spectroscopy", Perkin-Elmer Corporation, Physical Electronics Division, Eden Prairie, 1979.

[21]. D. A. Shirley, "High Resolution X-Ray Photoemission Spectrum of the Valence Band of Gold", Phys. Rev. B **5**, 4709-4714 (1972).

[22]. M.E. Davila, S.L. Molodtov, C. Laubschat, M.C. Asensio, "Surface-core-level shift photoelectron diffraction of Yb(111) films grown on W(110)", Surface and interface analysis **33**, 595-600 (2002).

Table 1. The coefficients of polynomial fits of *k* versus energy in the 48-190 and 210-1470 eV ranges

Range (eV)		E^1	E^0	E^{-1}	E^{-2}	E^{-3}	E^{-4}
k	48-190	6.086×10^{-4}	-0.3110	61.01	-5348	2.276×10^{5}	3.444×10^{6}
	210-1470		2.786×10^{-4}	-0.9815	1085	-1.817×10^{5}	1.389×10^{7}
δ	48-190		0.004158	-0.4455	146.3	4294	-1.342×10^{5}
	210-1470		-9.879×10^{-4}	2.010	-461.2	1.732×10^{5}	-2.172×10^{7}

Figure Captions

Fig. 1. (Color online) The transmittance of five Yb films with various thicknesses normalized to the transmittance of the substrate versus the logarithm of photon energy.

Fig. 2. (Color online) The transmittance of two current Yb films (lines without symbols) normalized to the transmittance of the substrate along with the transmittance of Yb films of close thicknesses taken from Ref. [2] (lines with symbols).

Fig. 3. (Color online) The logarithm of transmittance as a function of the film thickness at five different energies (symbols) and their fit with an exponential function (lines).

Fig. 4. (Color online) Log-log plot of the extinction coefficient of Yb as a function of photon energy. Literature data are also represented: Gribovskii et al.[3] in the 70-500 eV range, and Henke et al.[6] in the 30-1,700 eV range.

Fig. 5. (Color online) The extinction coefficient of Yb as a function of photon energy at $O_{2,3}$ edge and at the low absorption band below it. Literature data are also represented: Endriz and Spicer[1] and Larruquert et al.[2].

Fig. 6. (Color online) The extinction coefficient of Yb versus photon energy at $M_{4,5}$ edge. Henke data [6] are also represented.

Fig. 7. (Color online) The sets of *k* data that map a wide spectral range from the FIR to the γ rays using the current data along with the data of Endriz and Spicer[1], Larruquert et al.[2], Henke et al.[6], and Chantler et al.[17], and extrapolations in the two extremes.

Fig. 8. (Color online) Log-log plot of the refractive index of Yb as a function of photon energy. The data of Henke et al.[6] in the 30-1,700 eV range are also represented

Fig. 9. (Color online) δ=1-n of Yb as a function of photon energy at $O_{2,3}$ edge and at the low absorption band below it. Literature data are also represented: Endriz and Spicer[1], Larruquert et al.[2], and Henke et al.[6].

Fig. 10. (Color online) δ=1-n of Yb versus photon energy at $M_{4,5}$ edge. Henke data [6] are also represented.

Fig. 11. (Color online) Photemission measurements on three different films obtained at 650 eV. The electron analyzer was placed in normal emission.

Fig. 12. (Color online) Valence band photoemission spectra for three different Yb films, aligned at the Fermi level. The measurements were performed with electron analyzer in normal emission and with a photon energy of 150 eV.

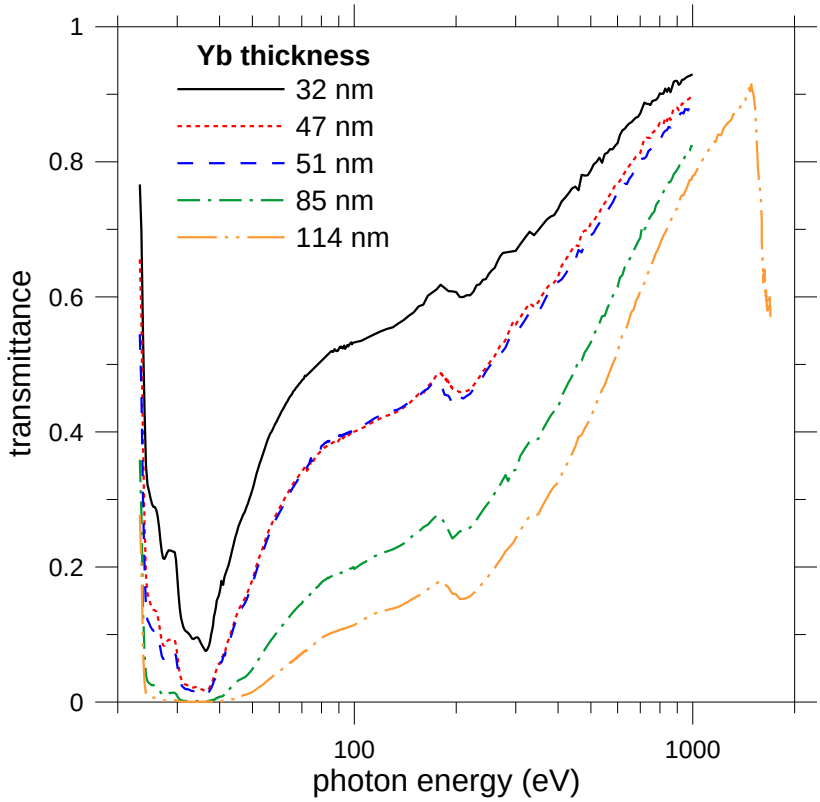
Yb thickness
32 nm
47 nm
51 nm
85 nm
114 nm
transmittance
photon energy (eV)
0
0.2
0.4
0.6
0.8
1
100
1000

Fig. 1.

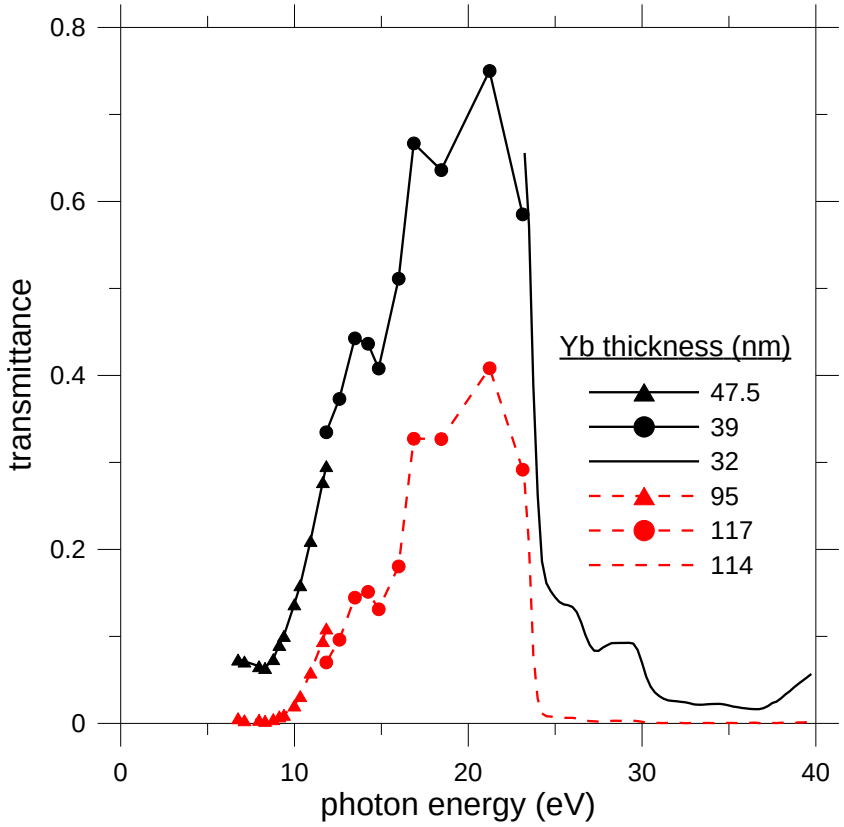
0.8
0.6
0.4
0.2
0
transmittance
0
10
20
30
40
photon energy (eV)
Yb thickness (nm)
47.5
39
32
95
117
114

Fig. 2.

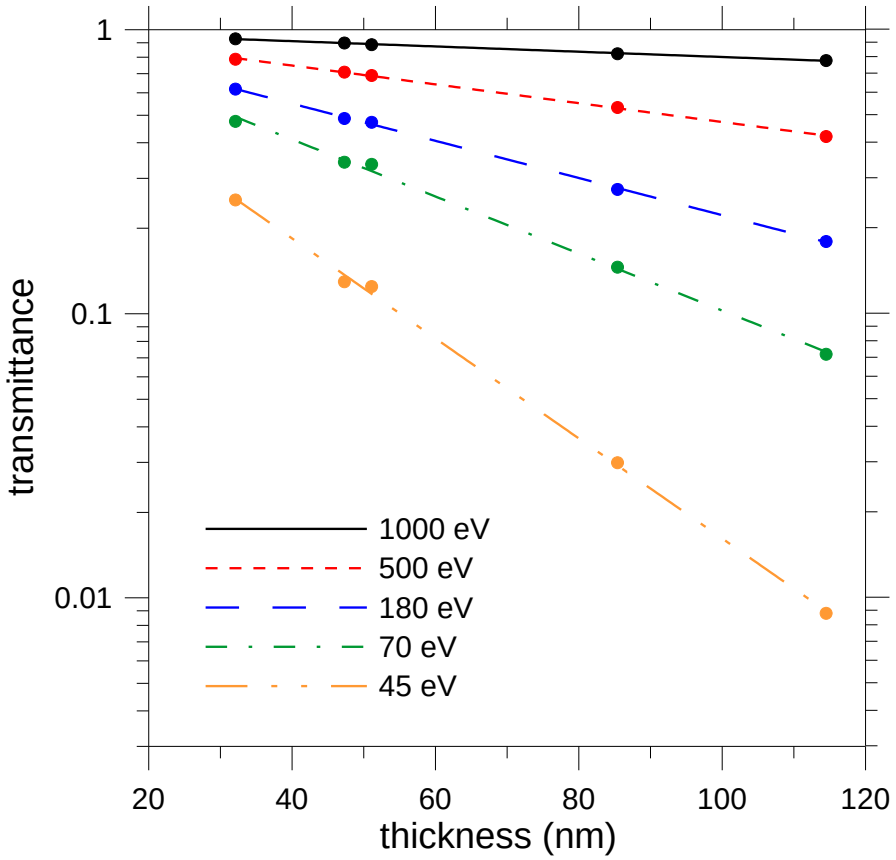
1
0.1
0.01
transmittance
20
40
60
80
100
120
thickness (nm)
1000 eV
500 eV
180 eV
70 eV
45 eV

Fig. 3.

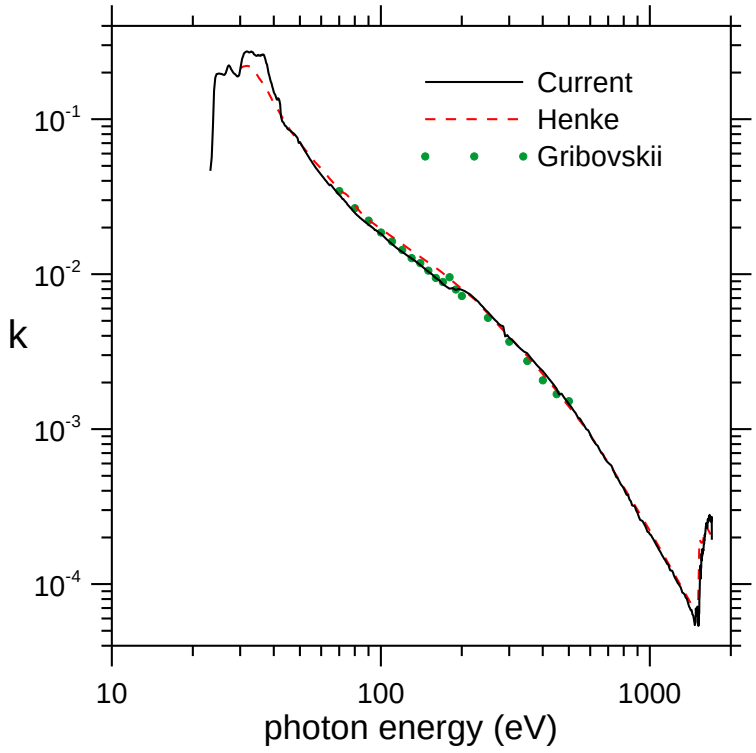
Current
Henke
Gribovskii
k
10^{-1}
10^{-2}
10^{-3}
10^{-4}
10
100
1000
photon energy (eV)

Fig. 4.

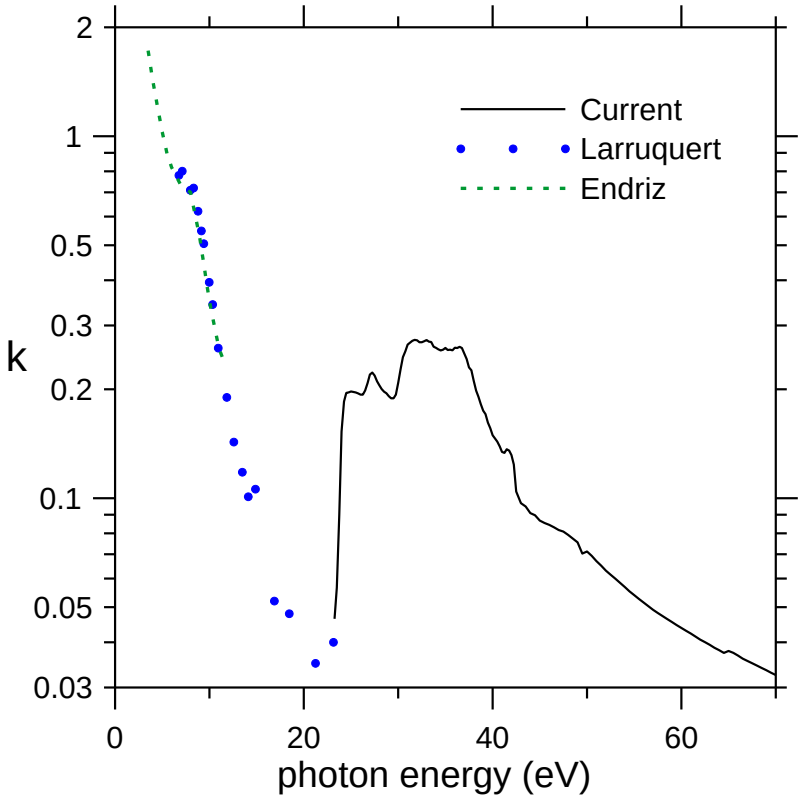
Current
Larruquert
Endriz
k
2
1
0.5
0.3
0.2
0.1
0.05
0.03
0
20
40
60
photon energy (eV)

Fig. 5.

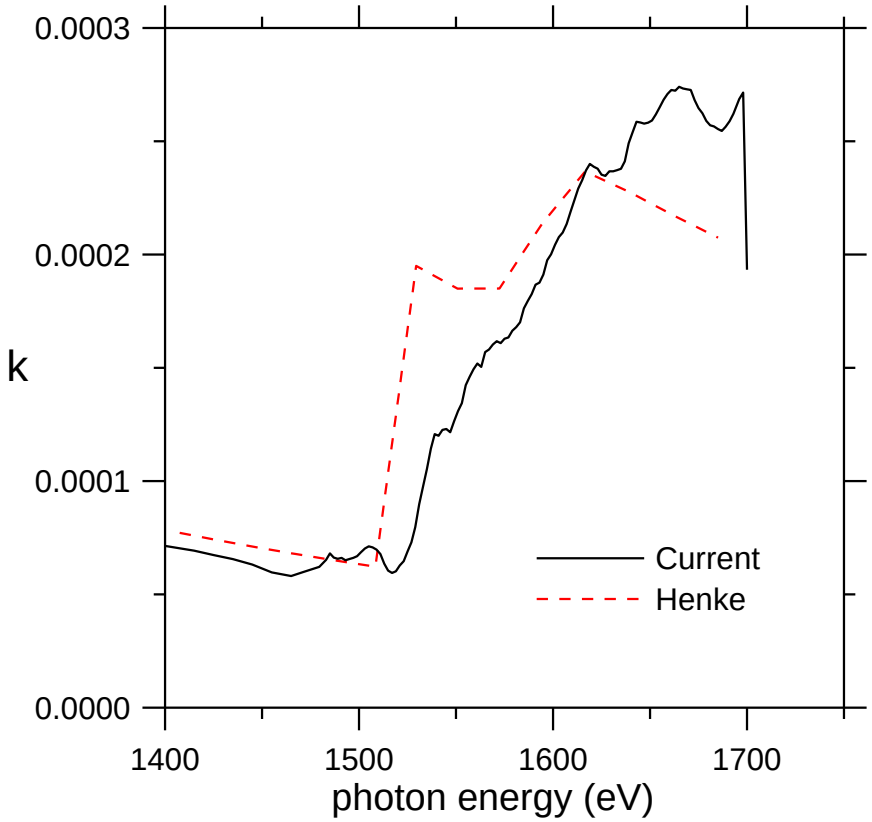
0.0003
0.0002
0.0001
0.0000
k
1400
1500
1600
1700
photon energy (eV)
Current
Henke

Fig. 6.

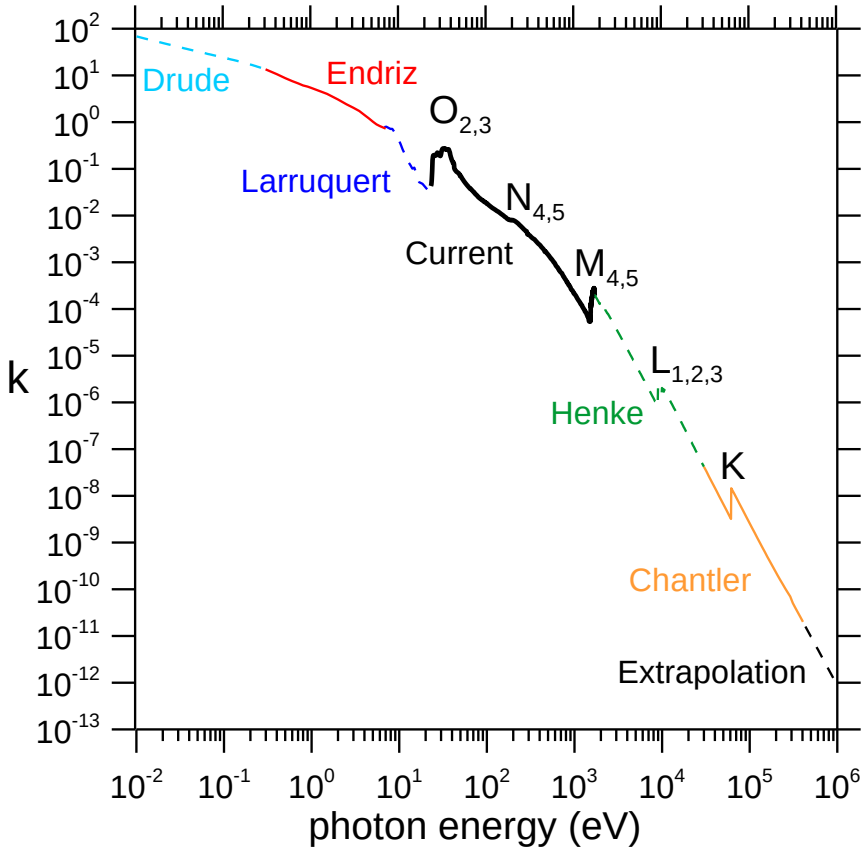
Drude
Endriz
O2,3
Larruquert
N4,5
Current
M4,5
L1,2,3
Henke
K
Chantler
Extrapolation
k
photon energy (eV)

Fig. 7.

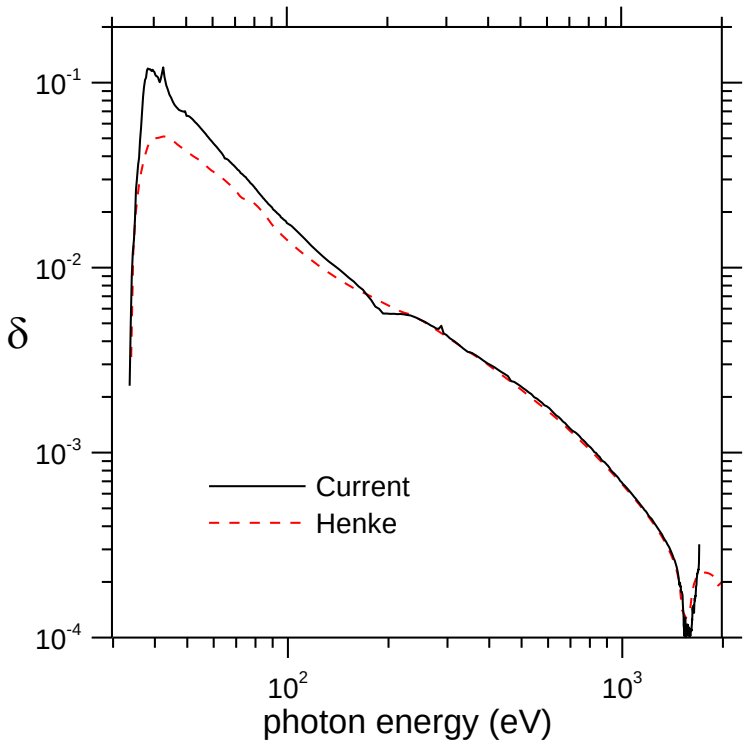

Fig. 8.

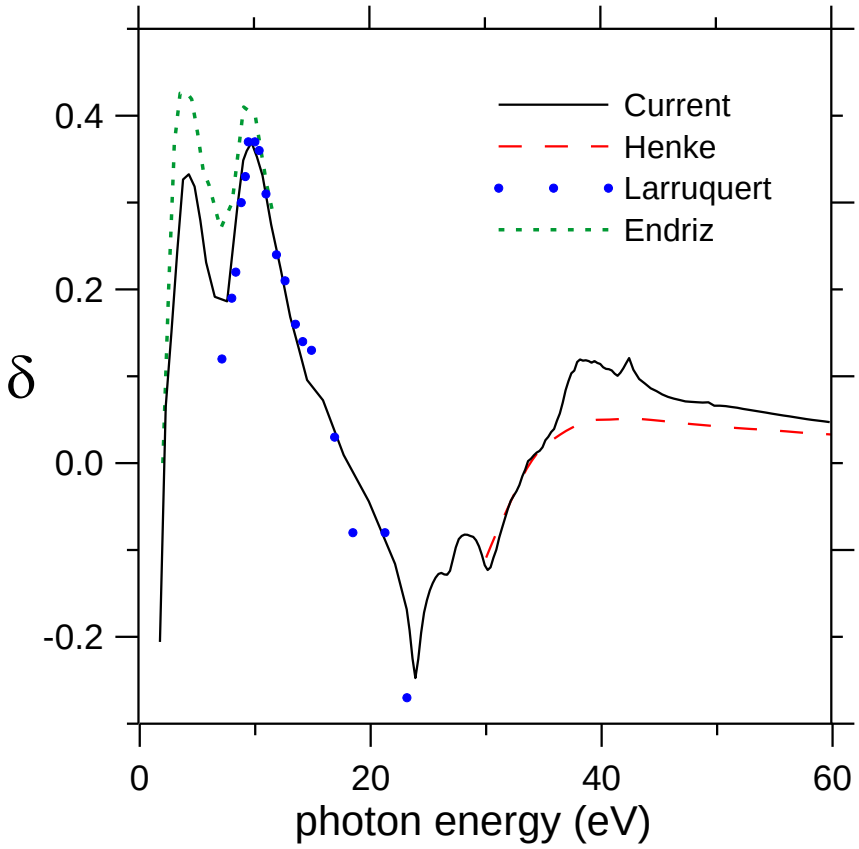
Current
Henke
Larruquert
Endriz
δ
0.4
0.2
0.0
-0.2
0
20
40
60
photon energy (eV)

Fig. 9.

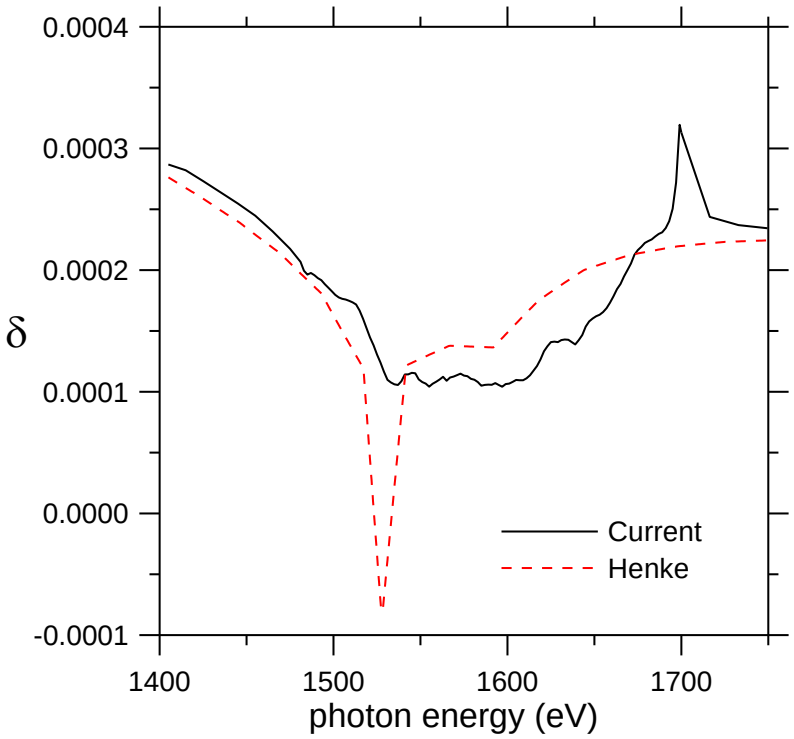
0.0004
0.0003
0.0002
0.0001
0.0000
-0.0001
δ
1400
1500
1600
1700
photon energy (eV)
Current
Henke

Fig. 10.

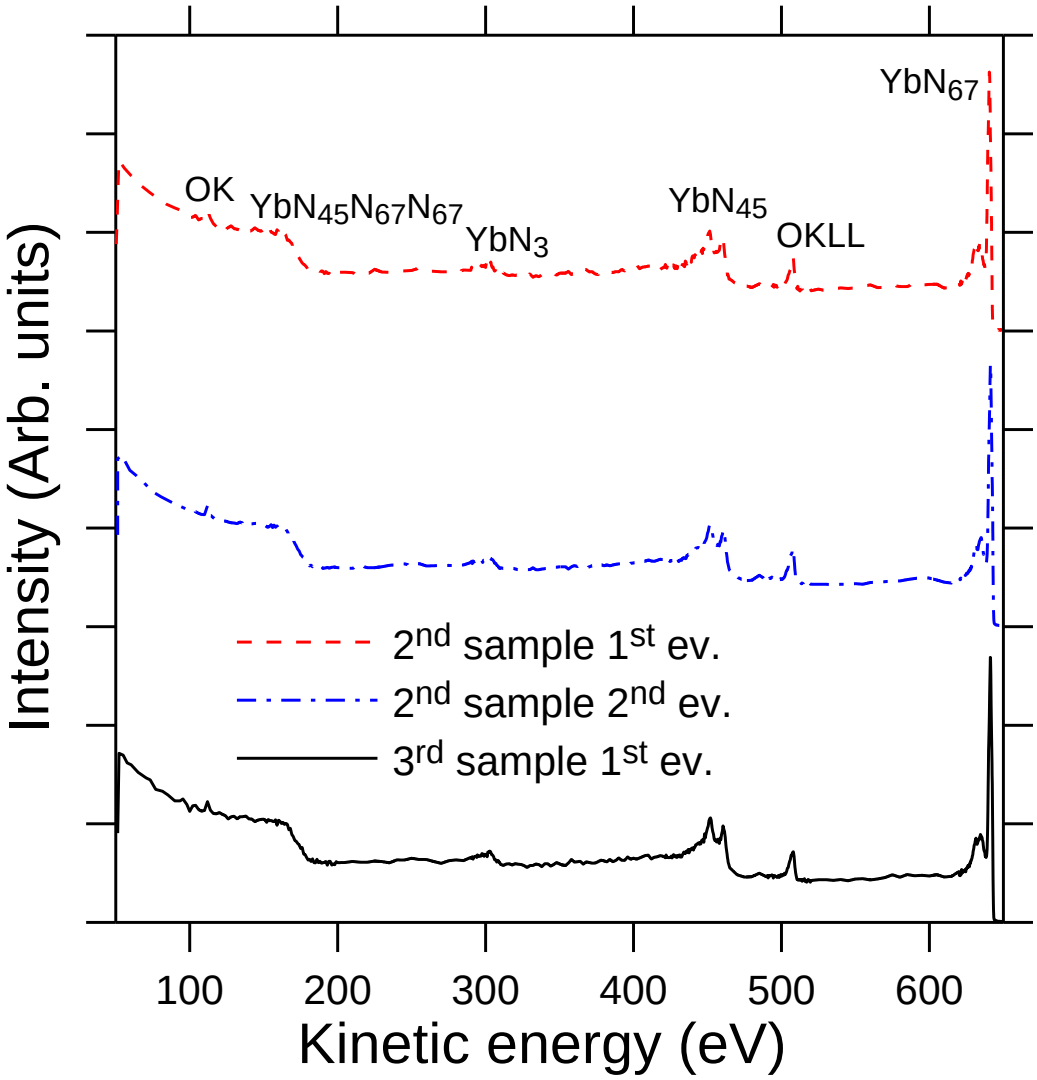
YbN67
OK
YbN45N67N67
YbN3
YbN45
OKLL
2nd sample 1st ev.
2nd sample 2nd ev.
3rd sample 1st ev.
Intensity (Arb. units)
100
200
300
400
500
600
Kinetic energy (eV)

Fig. 11.

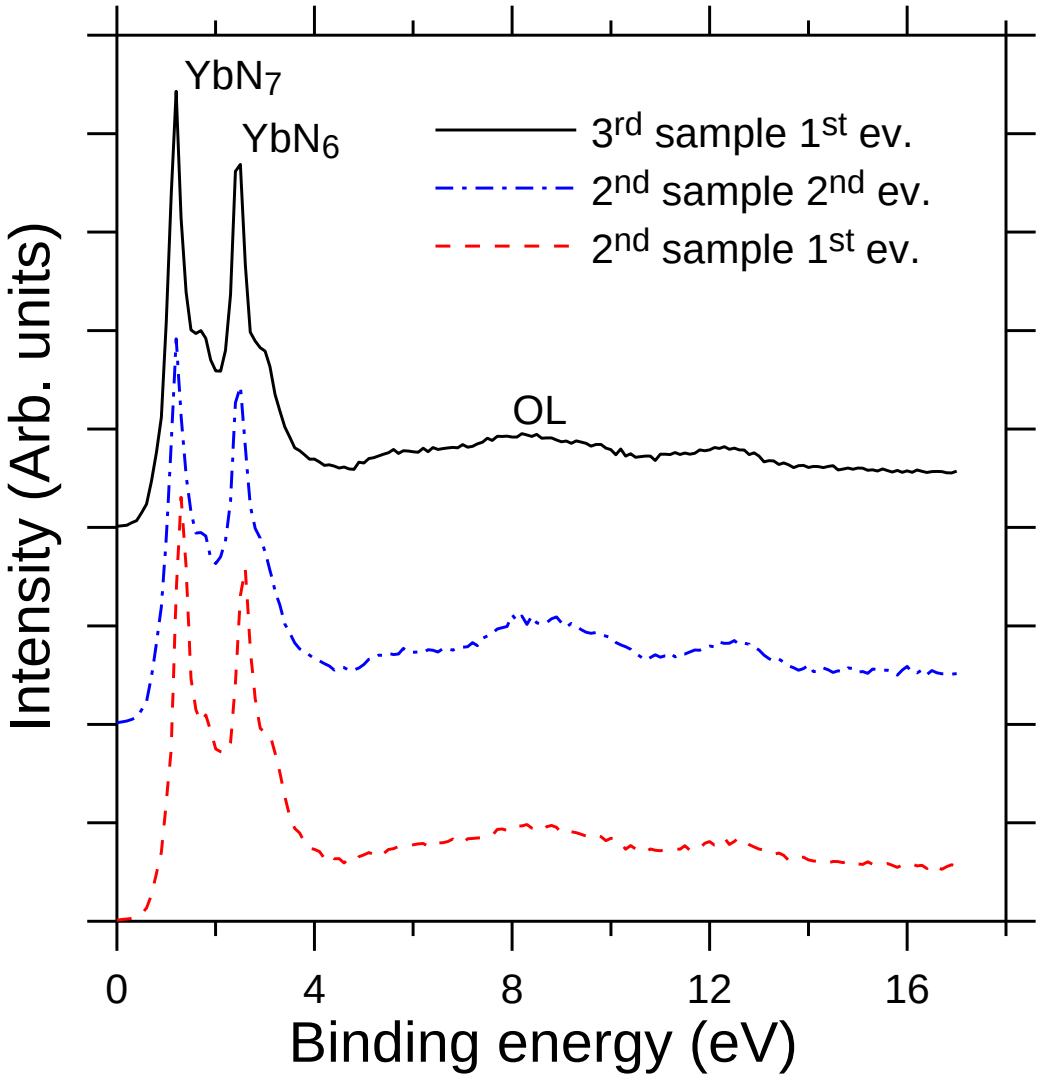
YbN7
YbN6
OL
3rd sample 1st ev.
2nd sample 2nd ev.
2nd sample 1st ev.
Intensity (Arb. units)
0
4
8
12
16
Binding energy (eV)

Fig. 12.